

Chikungunya Forecast of the Invasion Landscape in the Americas

T. Alex Perkins^{*1,2}, C. Jessica E. Metcalf³, Bryan T. Grenfell^{2,3}, Andrew J. Tatem^{2,4,5}

¹ Department of Biological Sciences and Eck Institute for Global Health, University of Notre Dame, Notre Dame, IN

² Fogarty International Center, National Institutes of Health, Bethesda, MD

³ Department of Ecology and Evolutionary Biology, Princeton University, Princeton, NJ

⁴ Department of Geography and Environment, University of Southampton, Southampton, UK

⁵ Flowminder Foundation, Stockholm, Sweden

* Author for correspondence; taperkins@nd.edu

1 Abstract

2 Background: Chikungunya is an emerging arbovirus that has caused explosive outbreaks in Africa and
3 Asia for decades and invaded the Americas just over a year ago. During this ongoing invasion, it has
4 spread to 45 countries where it has been transmitted autochthonously, infecting nearly 1.3 million people
5 in total.

6 Methods: Here, we made use of weekly, country-level case reports to infer relationships between trans-
7 mission and two putative climatic drivers: temperature and precipitation averaged across each country
8 on a monthly basis. To do so, we used a TSIR model that enabled us to infer a parametric relationship
9 between climatic drivers and transmission potential, and we applied a new method for incorporating a
10 probabilistic description of the serial interval distribution into the TSIR framework.

11 Results: We found significant relationships between transmission and linear and quadratic terms for tem-
12 perature and precipitation and a linear term for log incidence during the previous pathogen generation.
13 The lattermost suggests that case numbers three to four weeks ago are largely predictive of current case
14 numbers. This effect is quite nonlinear at the country level, however, due to an estimated mixing pa-
15 rameter of 0.74. Relationships between transmission and the climatic variables that we estimated were
16 biologically plausible and in line with expectations.

17 Conclusions: Our analysis suggests that autochthonous transmission of Chikungunya in the Americas
18 can be correlated successfully with putative climatic drivers, even at the coarse scale of countries and
19 using long-term average climate data. Overall, this provides a preliminary suggestion that successfully
20 forecasting the future trajectory of a Chikungunya outbreak and the receptivity of virgin areas may be

21 possible. Our results also provide tentative estimates of timeframes and areas of greatest risk, and our
22 extension of the TSIR model provides a novel tool for modeling vector-borne disease transmission.

23 **Funding Statement**

24 This work was funded by the Research and Policy for Infectious Disease Dynamics (RAPIDD) program
25 of the Science and Technology Directory, Department of Homeland Security, and Fogarty International
26 Center, National Institutes of Health, and by the Bill and Melinda Gates Foundation.

27 **Introduction**

28 Chikungunya is a painful affliction characterized by fever, arthralgia, and varying other symptoms [1,2].
29 It is caused by Chikungunya viruses (CHIKV), which are vectored between people primarily by either
30 *Aedes aegypti* or *Ae. albopictus* mosquitoes [3], depending on local vector ecology [1] and viral strain [4].
31 Outbreaks of Chikungunya have been highly explosive in a variety of contexts, ranging from tropical
32 islands [5] to temperate mainlands [6]. A large portion of cases are thought to be symptomatic [2],
33 making these outbreaks highly conspicuous, readily documentable, and of serious concern to public
34 health.

35 After its discovery in the 1950s, CHIKV was recognized as the etiological agent in outbreaks that
36 occurred throughout Africa, India, and Southeast Asia over the next several decades [1,7,8]. The last ten
37 years, however, have seen an alarming number of outbreaks globally, increased importation to new areas,
38 autochthonous transmission in Europe, and most recently invasion and establishment in the Americas
39 [8,9]. The first known autochthonous cases of CHIKV in the Americas were reported on December 5,
40 2013, and occurred on the island of Saint Martin in the Caribbean [10]. Its spread has since continued
41 throughout the Caribbean and into mainland South and North America [9]. The sequence of invasion
42 from one country in the Americas to another has received considerable attention from modelers and
43 appears to be quite predictable based on flight information, distance between countries, and climatic
44 suitability [11–14].

45 There have also been attempts to model the dynamics of the early stages of establishment within

46 a country, yielding estimates of probabilities of autochthonous transmission upon introduction [12, 15]
47 and the basic reproductive number R_0 , which is defined as the expected number of secondary infec-
48 tions caused by a single primary infection in a susceptible population [13]. Given the importance of the
49 mosquito vector in transmitting CHIKV, it is to be expected that the potential for autochthonous trans-
50 mission should depend greatly on local climatic and ecological conditions [16, 17] and that this potential
51 should therefore vary greatly in time and space. Efforts to quantify transmission potential to date have
52 relied on empirically derived descriptions of how different components of vectorial capacity depend on
53 weather-related covariates such as temperature and precipitation [12, 15], yet there has been very little
54 confirmation that these relationships are predictive of realized patterns of transmission. There has also
55 been scant consideration of susceptible depletion and its feedback onto transmission dynamics via herd
56 immunity, which should be important given the strong protective immunity that Chikungunya infection
57 confers [2, 3] and the high seroprevalence observed following outbreaks [5, 18, 19].

58 To fill these gaps among models that have been applied to the CHIKV epidemic in the Americas
59 thus far, we adapt the time-series susceptible-infectious-recovered (TSIR) framework [20] for modeling
60 CHIKV transmission dynamics. Originally developed for measles, the TSIR framework has been applied
61 to a variety of infectious diseases since [21–27] and offers a convenient way to model and estimate
62 susceptible build up and depletion and spatial and temporal variation in transmission. We describe our
63 application of this model to weekly case reports from countries in the Americas during the first year
64 of CHIKV invasion there. In doing so, we establish direct relationships between climatic drivers and
65 transmission, and we propose a platform for future work that will allow for inference of more nuanced
66 links between transmission and putative drivers and for forecasting the continued spread of CHIKV
67 throughout the Americas.

68 Methods

69 The goal of our analysis was to understand drivers of spatial and temporal variation in the potential for
70 autochthonous transmission, rather than drivers of pathogen movement and case importation. Conse-
71 quently, we used a model that accounts for the transmission process locally but that ignores the process
72 of pathogen movement between countries. The question of CHIKV dispersion and importation in the

73 Americas has been addressed previously [12–14] and is something that could be incorporated into our
74 framework in the future.

75 Model

76 Our model pertains to weekly incidence, which is denoted $I_{i,t}$ for week t in country i . We denote the
77 number of residents of i that are susceptible during week t as $S_{i,t}$. Given that the duration of infectious-
78 ness is expected to be about five days on average [12], the remaining proportion of the population is
79 assumed to have recovered and gained immunity within a week, so $R_{i,t} = N_i - S_{i,t} - I_{i,t}$. In doing
80 so, we assume that the total population size N_i is static and that births and deaths are negligible on the
81 timeframe over which the model is applied. The duration of the incubation period of the virus in humans
82 is expected to be between three and seven days [2], so we assume that cases in week t derive from sus-
83 ceptible people in week $t - 1$. Due to the presence of a vector, the period of time separating successive
84 cases, or the serial interval, is relatively prolonged and variable. To account for this, we introduce a mod-
85 ification to the standard TSIR framework that allows for an arbitrary specification of the serial interval
86 distribution.

87 To account for this distributed time lag between successive cases, we treated the effective number of
88 infectious people during the time interval in which transmission occurs as

$$I'_{i,t} = \sum_{n=1}^5 \omega_n (I_{i,t-n} + \iota_{i,t-n}), \quad (1)$$

89 where $I_{i,t-n}$ are cases acquired locally and $\iota_{i,t-n}$ are imported cases. The coefficients that weight con-
90 tributions of infectious people n weeks ago to infections in the current week are calculated according
91 to

$$\omega_n = \frac{1}{7} \int_{7(n-1)}^{7n} F(\tau + 7) - F(\tau) d\tau, \quad (2)$$

92 where F is the distribution function of the serial interval and τ is a dummy variable. This formulation
93 assumes that the timing of cases within a week is uniform and that a case on day t arose from a case
94 on day $t - \tau$ with probability $f(\tau)$, where f is the density function corresponding to F . We chose
95 a functional form and parameters for f and F consistent with a previously published serial interval

96 distribution for CHIKV [13]. Assuming a gamma distribution and applying the method of moments to
97 the mean and standard deviation reported in [13], we used values of the shape and rate parameters for the
98 serial interval distribution of 14.69 and 0.64, respectively. Applying these numbers to eqn. (2) using the
99 integrate function in R [28] and normalizing resulted in values of $\omega_{1,\dots,5} = 0.011, 0.187, 0.432, 0.287,$
100 and 0.083. A schematic depiction of the calculation of $I'_{i,t}$ based on $I_{i,t-n}$ and ω_n is shown in Fig. 1.

101 Consistent with a frequency-dependent formulation of the TSIR model for directly transmitted pathogens,
102 e.g., [23], we modeled the dynamics of the infectious class as

$$I_{i,t} = \beta_{i,t} \frac{I'_{i,t}^\alpha}{N_i} S_{i,t-1}, \quad (3)$$

103 where $\beta_{i,t}$ is a transmission coefficient for country i on week t . Under this formulation, $\beta_{i,t}$ is related to
104 the basic reproductive number, R_0 , in country i in week t by

$$R_0(i, t) = \sum_{n=1}^5 \omega_n \beta_{i,t+n}. \quad (4)$$

105 The transmission coefficient $\beta_{i,t}$ is assumed to implicitly account for a number of factors, including
106 the probabilities of transmission from infectious people to susceptible mosquitoes and from infectious
107 mosquitoes to susceptible people, the ratio of mosquitoes to people, mosquito longevity beyond the
108 pathogen's incubation period in the mosquito, and the rate at which adult female mosquitoes feed on
109 blood [27]. Another assumption of this formulation is that encounters between mosquitoes and people
110 are well mixed, which while potentially problematic for modeling mosquito-borne pathogen transmission
111 [29], can be accounted for phenomenologically by inclusion of the mixing parameter $\alpha \in [0, 1]$ [30, 31].
112 Dynamics of the susceptible and recovered classes follow from eqn. (3), the assumption of recovery
113 within one week, and the assumption of a static population, yielding $S_{i,t} = S_{i,t-1} - I_{i,t}$ and $R_{i,t} =$
114 $R_{i,t-1} + I_{i,t-1}$.

115 Data

116 The centerpiece of our analysis were weekly numbers of Chikungunya cases on a national scale for coun-
117 tries in the Americas. At the time that we conducted our analysis, there were 1,293,836 cases reported
118 over 61 weeks in 50 countries. Of these, 1,185,728 were suspected cases, each of which corresponded

119 to an individual who sought medical treatment and was diagnosed with Chikungunya based on their
120 presentation of symptoms. An additional 101,651 cases were additionally confirmed by either PCR,
121 serology, or laboratory culture. The remaining 6,457 cases were deemed imported based on travel his-
122 tories. We obtained data for the first ten weeks from Project Tycho [32], which in turn obtained them
123 from the Agence Régionale de Santé, and for the remaining 51 weeks from the Pan American Health
124 Organization’s website.

125 In addition to case numbers, we utilized data on synoptic monthly temperature and precipitation av-
126 eraged at a national scale from $1 \text{ km} \times 1 \text{ km}$ gridded data. These data were obtained from WorldClim
127 (www.worldclim.org), and represent interpolated meteorological station data on temperature and precipi-
128 tation from the 1950-2000 period, processed to create synoptic monthly averages that represent “typical”
129 conditions [33]. To obtain weekly temperature and precipitation values, we assigned monthly values to
130 weeks that fell entirely within a month and took a weighted average in the event that a week spanned two
131 months. We obtained country-level population estimates from the Central Intelligence Agency World
132 Factbook (<https://www.cia.gov/library/publications/the-world-factbook/rankorder/2119rank.html>).

133 **Estimating drivers of transmission**

134 Given data on weekly cases and a generative model for those data, we estimated the mixing parameter
135 α and relationships between local transmission coefficients $\beta_{i,t}$ and two putative drivers of transmission:
136 temperature and precipitation. To do so, we rearranged terms in eqn. (3) to arrive at the regression
137 equation

$$\ln(I_{i,t}) - \ln(S_{i,t-1}) + \ln(N_i) = \ln(\beta_{i,t}) + \alpha \ln(I'_{i,t}), \quad (5)$$

138 where

$$\ln(\beta_{i,t}) = f(T'_{i,t}, P'_{i,t}) + \epsilon, \quad (6)$$

139 $T'_{i,t}$ and $P'_{i,t}$ are moving averages of temperature and precipitation in country i in weeks $t - 5$ through
140 $t - 1$, and ϵ is a normally distributed random variable with mean zero. Regarding the functional form of
141 $f(T'_{i,t}, P'_{i,t})$, we assumed

$$f(T'_{i,t}, P'_{i,t}) = a_0 + a_1 T'_{i,t} + a_2 P'_{i,t} + a_3 {T'_{i,t}}^2 + a_4 {P'_{i,t}}^2. \quad (7)$$

142 To select among subsets of this model with the possibility of some coefficients equal to zero, we used
 143 the stepAIC function in the MASS package [34] in R [28]. This applied both forward and backward
 144 selection to yield a model minimizing the Akaike Information Criterion and estimates of best-fit values
 145 of its coefficients. Because weeks in which either $I_{i,t}$ or $I'_{i,t}$ equalled zero were not informative in
 146 the regression, we performed this analysis only for country-weeks in which these conditions were not
 147 violated. We furthermore excluded weeks for which $I'_{i,t} < 1$ to preserve a single case as a lower bound
 148 for generating autochthonous transmission. We considered $I_{i,t}$ to include both suspected and confirmed
 149 cases and $\iota_{i,t}$ to represent imported cases. To examine patterns of variation in transmission predicted by
 150 the best-fit model, we computed values of $\beta_{i,t}$ based on the fitted model for 53 countries in the Americas
 151 in each of 52 weeks in a year with a typical climate regime.

152 Results

153 Performing a regression of incidence against temperature and precipitation according to eqns. (5)-(7)
 154 yielded significant associations between transmission and linear and quadratic terms for temperature and
 155 precipitation ($F_{5,478} = 254.6, p < 2.2 \times 10^{-16}$) (Table 1). There was likewise strong support for a mixing
 156 parameter less than one, with a best-fit estimate of $\alpha = 0.74$ ($t = 22.58, p < 2 \times 10^{-16}$). Although
 157 models with fewer terms were fitted and compared, the full model in eqn. (7) had the lowest AIC value
 158 and was thus supported as the best model by that criterion. Partial residual plots provided an indication
 159 of the extent to which each variable accounted for different portions of overall residual variation (Fig. 2).
 160 Overall, the model accounted for 72.4% of variation in incidence among country-weeks, as determined
 161 by adjusted R^2 (Fig. 3).

162 The fitted model predicted that the transmission coefficient, and R_0 , should be highest at a temper-
 163 ature of 25 °C and monthly precipitation of 206 mm (Fig. 4). Most country-weeks that experienced
 164 autochthonous transmission of CHIKV fell within approximately 3 °C of the temperature optimum but
 165 across a large swath of monthly precipitation values (Figs. 2 & 4). Applying the best-fit model to tem-

166 perature and precipitation data from all 52 weeks in 53 countries showed that the timing and duration
167 of high-transmission seasons are projected to vary substantially across countries (Fig. 5). Such differ-
168 ences mimic clear latitudinal patterns in the seasonality of temperature and, in some areas, precipitation.
169 In general, countries at high and mid latitudes were projected to have the highest potential for Chikun-
170 gunya transmission from April through November and countries at low latitude from November through
171 April, although there were of course some exceptions to these general patterns (Fig. 5). In addition to
172 geographic variation in seasonality, the best-fit model also projected that mid-latitude countries should
173 generally have higher transmission potential than those at latitudinal extremes (Fig. 6-9). Some outliers
174 included countries with substantial areas of high-altitude terrain, such as Ecuador and Peru.

175 Discussion

176 The ongoing epidemic of Chikungunya throughout the Americas is nearing 1.3 million cases and is
177 showing no signs of abating. In many ways, the present time is a critical juncture in the pathogen's
178 invasion and in the public's response to it. Because CHIKV has been spreading in the Americas for over
179 a year, there are sufficient data to begin analyzing its spread and learning about drivers thereof, as we
180 have demonstrated in the present analysis. At the same time, there are many more millions of people
181 at risk, so improving the capacity to forecast, prepare for, and mitigate outbreaks is paramount. In the
182 present study, we have made several advances towards this goal.

183 Building on successful application of TSIR models to childhood and other diseases [20–27], we have
184 proposed this framework as a potentially useful tool for modeling Chikungunya transmission. Appli-
185 cation of this method to Chikungunya is reasonable based on a number of similarities between these
186 pathogens, including the development of strong protective immunity, a reasonably short period of infec-
187 tiousness, and the potential to rapidly infect (and induce immunity in) large numbers of people. At the
188 same time, application of this method to Chikungunya requires some important considerations. First, in-
189 corporation of frequency-dependent transmission and dependence on climatic drivers is critical [22, 24].
190 Second, the serial interval for vector-borne diseases is necessarily much longer than it is for directly
191 transmitted diseases due to incubation of the pathogen in the vector and the possibility of prolonged
192 transmission over multiple feeding cycles of the vector. By proposing a formulation of the TSIR model

193 similar to an autoregressive moving average time series model, we have provided a new way to accom-
194 modate this important feature of vector-borne disease biology without unnecessarily aggregating data
195 temporally and thus potentially compromising information content of the data.

196 A powerful feature of the TSIR framework is that it reveals variation in transmission and provides
197 a clear and uncomplicated way of statistically associating that variation with putative drivers of trans-
198 mission. Our analysis of 484 country-weeks of data indicated that there were significant relationships
199 between country-level transmission of CHIKV and typical temperature and precipitation regimes. The
200 concordance of these inferred relationships with previous knowledge is encouraging, because these rela-
201 tionships were apparent in our analysis only because of their demonstrated relationship with variation in
202 transmission and not because of a priori assumptions. The inferred association between temperature and
203 transmission is reasonable due to its height in the 20-30 °C range, although the inferred optimum of 25
204 °C is lower than some studies would suggest [12, 16] but consistent with others [17]. The relationship
205 between precipitation and transmission that we inferred is also biologically plausible, as extremely low
206 precipitation would make for insufficient breeding habitats, and too much could flood eggs from breeding
207 habitats or make people less likely to store water and thereby reduce habitat for the aquatic stages of the
208 *Aedes aegypti* mosquito that has been implicated in the current outbreak. For both of these relationships,
209 it is worth bearing in mind that values of the covariate climate data that we used reflect national and long-
210 term averages, and values in more localized areas where transmission occurs will vary considerably and
211 exhibit inter-annual variations. Consequently, our estimates of optimal conditions for transmission are
212 not directly comparable to estimates derived from local studies. Nonetheless, the relationships that we
213 inferred are biologically plausible and, in the spirit of forecasting, predictive of variation in transmission.

214 Applying inferred relationships between transmission and putative drivers thereof to comprehensive
215 spatial and temporal data on those drivers offers a means to anticipate future hotspots of transmission
216 in space and time. On the one hand, such predictions could provide local public health agencies with
217 an estimate of timeframes over which they may be more likely to experience outbreaks due to elevated
218 autochthonous transmission, allowing time to mobilize resources for increased vector control or hospital
219 beds [35]. On the other hand, considering these predictions in a regional context could provide insight
220 about when and from where imported cases are likely to appear. Combining this information with knowl-

221 edge of when the potential for local transmission should be highest would be most valuable [36]. Patterns
222 of coupling in the timing of heightened transmission between different areas also have implications for
223 regional persistence [37, 38]. Provided that case importation from country to country is sufficiently fre-
224 quent, the varying seasonality of heightened transmission across latitudes could very well make regional
225 persistence more likely than otherwise, and regional control more challenging in the absence of coor-
226 dinated efforts [25, 39, 40]. One important caveat to bear in mind, however, is that realized patterns
227 of transmission depend not just on the potential for transmission but also on the presence of sufficient
228 numbers of infectious and susceptible individuals in the same place at roughly the same time [26]. The
229 landscape of Chikungunya transmission in the Americas is therefore likely to remain highly dynamic as
230 its invasion progresses.

231 In addition to providing insight about relative patterns of transmission potential in space and time, our
232 results also provide estimates of the magnitude of transmission potential by way of the basic reproductive
233 number R_0 . In mid-latitude locations where transmission potential is expected to be greatest, our pro-
234 jections of yearly averages of R_0 range 4-7 and projections of yearly maxima in some countries exceed
235 8. On the other extreme, for high- and low-latitude countries, such as Canada, the United States, Chile,
236 Argentina, and the Falkland Islands, we projected weekly values of R_0 below 1 for nearly all weeks of
237 a typical year. Given that our analysis did not account for variation below the level of countries, there
238 could very well be local areas within some of these countries with $R_0 > 1$ for much of the year. On the
239 whole, these estimates appear somewhat high compared to previous estimates, although not completely
240 out of the realm of possibility. Using different methodology, estimates of R_0 early in the invasion of
241 CHIKIV in the Americas ranged 2-4 based on data from Guadeloupe, Martinique, and Saint Martin [13].
242 Estimates based on data from outside the Americas [41, 42] or on temperature-dependent parameteriza-
243 tion of an a priori formula [12] were in the range of 4-7. It is also relevant to note that estimates of R_0
244 for dengue, which is ecologically very similar to Chikungunya, typically range 2-6 [43], with substantial
245 seasonal variation having been noted [44]. One reason that our estimates may skew high is due to our
246 relatively low estimate of $\alpha = 0.74$ (cf. $\alpha \approx 0.9$ for dengue in Thailand [27]) and an inherent tradeoff
247 between mixing and transmission [29]. It is also possible that our estimates were affected by systematic
248 errors in the data, such as reporting a backlog of cases in a single week, or failing to detect low numbers

249 of cases early in the invasion of a given country.

250 As encouraging as it was that we were able to infer biologically plausible relationships between
251 transmission and putative drivers based directly on weekly case reports, there are a number of limi-
252 tations of the data and model that we used. Foremost among these limitations is the coarse spatial
253 resolution of both. Whether it be at the level of a state or municipality, spatial disaggregation of the
254 data would be extremely valuable for efforts to model and forecast CHIKV transmission [29, 45], be-
255 cause the data could then be linked with much more relevant information about putative drivers [46].
256 Even so, developments in modeling methodology to account for subnational heterogeneity in generating
257 national-level patterns could possibly help in this regard. In addition to spatial and temporal resolution
258 and other issues of data quality, coordinated efforts to make case data publicly available, and to do so
259 in usable formats (e.g., csv rather than pdf files), would accelerate the development and application of
260 innovative modeling and forecasting frameworks [32]. The same is true for data about covariates, such
261 as various attributes of temperature, precipitation, humidity, land cover, human population density, and
262 others that currently require assembling from a wide range of disparate sources as well as substantial
263 processing to make them coherent and comparable. Lastly, integrating data and models into readily
264 usable, interactive tools that enable real-time forecasting and decision making should represent a penul-
265 timate goal of these activities, as exemplified by efforts by the United States Centers for Disease Control
266 (<http://www.cdc.gov/chikungunya/modeling/>).

267 **Acknowledgements**

268 Thanks to Ethan Holland for assistance with data entry and management.

269 **References**

270 [1] Powers AM, Logue CH (2007) Changing patterns of Chikungunya virus: re-emergence of a
271 zoonotic arbovirus. *Journal of General Virology* 88: 2363–77.

272 [2] Staples JE, Breiman RF, Powers AM (2009) Chikungunya fever: an epidemiological review of a
273 re-emerging infectious disease. *Clinical Infectious Diseases* 49: 942–8.

- 274 [3] Pialoux G, Gaüzère BA (2007) Chikungunya, an epidemic arbovirosis. Lancet Infectious Diseases
275 7: 319–327.
- 276 [4] Tsetsarkin KA, Vanlandingham DL, McGee CE, Higgs S (2007) A single mutation in Chikungunya
277 virus affects vector specificity and epidemic potential. PLOS Pathogens 3: e201.
- 278 [5] Josseran L, Paquet C, Zehgnoun A, Caillere N, Le Tertre A, et al. (2006) Chikungunya disease
279 outbreak, reunion island. Emerging Infectious Diseases 12: 1994.
- 280 [6] Rezza G, Nicoletti L, Angelini R, Romi R, Finarelli A, et al. (2007) Infection with chikungunya
281 virus in italy: an outbreak in a temperate region. Lancet 370: 1840–1846.
- 282 [7] Weaver SC, Reisen WK (2010) Present and future arboviral threats. Antiviral Research 85: 328–
283 45.
- 284 [8] Weaver SC (2014) Arrival of Chikungunya virus in the new world: prospects for spread and impact
285 on public health. PLOS Neglected Tropical Diseases 8: e2921.
- 286 [9] Staples JE, Fischer M (2014) Chikunguna virus in the Americas – What a vector borne pathogen
287 can do. New England Journal of Medicine 371: 887–9.
- 288 [10] Leparc-Goffart I, Nougairede A, Cassadou S, Prat C, de Lamballerie X (2014) Chikungunya in the
289 Americas. Lancet 383: 514.
- 290 [11] Tatem AJ, Huang Z, Das A, Qi Q, Roth J, et al. (2012) Air travel and vector-borne disease move-
291 ment. Parasitology 139: 1816–1830.
- 292 [12] Johansson MA, Powers AM, Pesik N, Cohen NJ, Staples JE (2014) Nowcasting the spread of
293 Chikungunya virus in the Americas. PLOS One 9: e104915.
- 294 [13] Cauchemez S, Ledrans M, Poletto C, Quenel P, Valk HD, et al. (2014) Local and regional spread of
295 Chikungunya fever in the Americas. Eurosurveillance 19: 20854.
- 296 [14] Khan K, Bogoch I, Brownstein JS, Miniota J, Nicolucci A, et al. (2014) Assessing the Origin of
297 and Potential for International Spread of Chikungunya Virus from the Caribbean. PLOS Currents
298 Outbreaks 1: 1–11.

- 299 [15] Ruiz-Moreno D, Vargas IS, Olson KE, Harrington LC (2012) Modeling dynamic introduction of
300 Chikungunya virus in the United States. PLOS Neglected Tropical Diseases 6: e1918.
- 301 [16] Chan M, Johansson MA (2012) The incubation periods of dengue viruses. PLOS One 7: e50972.
- 302 [17] Brady OJ, Golding N, Pigott DM, Kraemer MUG, Messina JP, et al. (2014) Global temperature
303 constraints on *Aedes aegypti* and *Ae. albopictus* persistence and competence for dengue virus trans-
304 mission. Parasites & Vectors 7: 338.
- 305 [18] Sissoko D, Moendandze A, Malvy D, Giry C, Ezzedine K, et al. (2008) Seroprevalence and risk
306 factors of chikungunya virus infection in Mayotte, Indian Ocean, 2005-2006: a population-based
307 survey. PLOS One 3: e3066.
- 308 [19] Schwarz NG, Germann M, Randriamampionona N, Bialonski A, Maus D, et al. (2012) Seropreva-
309 lence of antibodies against Chikungunya, dengue, and Rift Valley fever viruses after febrile illness
310 outbreak, Madagascar. Emerging Infectious Diseases 18.
- 311 [20] Finkenstädt BF, Grenfell BT (2000) Time series modelling of childhood diseases: a dynamical
312 systems approach. Journal of the Royal Statistical Society Series C 49: 187–205.
- 313 [21] Grenfell BT, Björnstad ON, Kappey J (2001) Travelling waves and spatial hierarchies in measles
314 epidemics. Nature 414: 716–23.
- 315 [22] Koelle K, Pascual M (2004) Disentangling extrinsic from intrinsic factors in disease dynamics: a
316 nonlinear time series approach with an application to cholera. American Naturalist 163: 901–13.
- 317 [23] Xia Y, Björnstad ON, Grenfell BT (2004) Measles metapopulation dynamics: a gravity model for
318 epidemiological coupling and dynamics. American Naturalist 164: 267–81.
- 319 [24] Pascual M, Cazelles B, Bouma MJ, Chaves LF, Koelle K (2008) Shifting patterns: malaria dynam-
320 ics and rainfall variability in an African highland. Proceedings of the Royal Society Series B 275:
321 123–32.

- 322 [25] Metcalf CJE, Björnstad ON, Ferrari MJ, Klepac P, Bharti N, et al. (2010) The epidemiology of
323 rubella in Mexico: seasonality, stochasticity and regional variation. *Epidemiology and Infection*
324 139: 1–10.
- 325 [26] Metcalf CJE, Munayco CV, Chowell G, Grenfell BT, Björnstad ON (2011) Rubella metapopulation
326 dynamics and importance of spatial coupling to the risk of congenital rubella syndrome in Perú.
327 *Journal of the Royal Society Interface* 8: 369–76.
- 328 [27] Reich NG, Shrestha S, King AA, Rohani P, Lessler J, et al. (2013) Interactions between serotypes of
329 dengue highlight epidemiological impact of cross-immunity. *Journal of the Royal Society Interface*
330 10: 20130414.
- 331 [28] R Core Team (2014) R: A Language and Environment for Statistical Computing. R Foundation for
332 Statistical Computing, Vienna, Austria. URL <http://www.R-project.org/>.
- 333 [29] Perkins TA, Scott TW, Le Menach A, Smith DL (2013) Heterogeneity, mixing, and the spatial
334 scales of mosquito-borne pathogen transmission. *PLOS Computational Biology* 9: e1003327.
- 335 [30] Liu W, Hethcote HW, Levin SA (1987) Dynamical behavior of epidemiological models with non-
336 linear incidence rates. *Journal of Mathematical Biology* 25: 359–380.
- 337 [31] Glass K, Xia Y, Grenfell B (2003) Interpreting time-series analyses for continuous-time biological
338 models: measles as a case study. *Journal of Theoretical Biology* 223: 19–25.
- 339 [32] van Panhuis WG, Grefenstette J, Jung SY, Chok NS, Cross A, et al. (2013) Contagious diseases in
340 the United States from 1888 to the present. *New England Journal of Medicine* 369: 2152–2158.
- 341 [33] Hijmans RJ, Cameron SE, Parra JL, Jones PG, Jarvis A (2005) Very high resolution interpolated
342 climate surfaces for global land areas. *International Journal of Climatology* 25: 1965–1978.
- 343 [34] Venables WN, Ripley BD (2002) Modern Applied Statistics with S. New York: Springer, fourth
344 edition. URL <http://www.stats.ox.ac.uk/pub/MASS4>. ISBN 0-387-95457-0.
- 345 [35] Hii Y, Rocklöv J, Wall S, Ng L (2012) Optimal lead time for dengue forecast. *PLOS Neglected
346 Tropical Diseases* 6: e1848.

- 347 [36] Chowell G, Cazelles B, Broutin H, Munayco CV (2011) The influence of geographic and climate
348 factors on the timing of dengue epidemics in Perú, 1994-2008. *BMC Infectious Diseases* 11: 164.
- 349 [37] Bolker B, Grenfell B (1995) Space, persistence and dynamics of measles epidemics. *Philosophical
350 Transactions of the Royal Society of London Series B* 348: 309–320.
- 351 [38] Grenfell B, Harwood J (1997) (Meta) population dynamics of infectious diseases. *Trends in Ecol-
352 ogy & Evolution* 12: 395–399.
- 353 [39] Bahl J, Nelson MI, Chan KH, Chen R, Vijaykrishna D, et al. (2011) Temporally structured metapop-
354 ulation dynamics and persistence of influenza A H3N2 virus in humans. *Proceedings of the National
355 Academy of Sciences* 108: 19359–19364.
- 356 [40] Klepac P, Laxminarayan R, Grenfell BT (2011) Synthesizing epidemiological and economic optima
357 for control of immunizing infections. *Proceedings of the National Academy of Sciences* 108:
358 14366–14370.
- 359 [41] Yakob L, Clements ACA (2013) A mathematical model of Chikungunya dynamics and control: the
360 major epidemic on Réunion Island. *PLOS One* 8: e57448.
- 361 [42] Robinson M, Conan A, Duong V, Ly S, Ngan C, et al. (2014) A model for a Chikungunya outbreak
362 in a rural Cambodian setting: implications for disease control in uninfected areas. *PLOS Neglected
363 Tropical Diseases* 8: e3120.
- 364 [43] Johansson MA, Hombach J, Cummings DAT (2011) Models of the impact of dengue vaccines: A
365 review of current research and potential approaches. *Vaccine* 29: 5860–5868.
- 366 [44] Reiner RC, Stoddard ST, Forshey BM, King AA, Ellis AM, et al. (2014) Time-varying, serotype-
367 specific force of infection of dengue virus. *Proceedings of the National Academy of Sciences* 111:
368 E2694–702.
- 369 [45] Mills HL, Riley S (2014) The spatial resolution of epidemic peaks. *PLOS Computational Biology*
370 10: e1003561.

371 [46] Johansson MA, Dominici F, Glass GE (2009) Local and global effects of climate on dengue trans-
372 mission in Puerto Rico. PLOS Neglected Tropical Diseases 3: e382.

373 **Tables**

Term	Parameter	Estimate	Std. Error	t	p
Intercept	a_0	-25.71	6.70	-3.840	1.4×10^{-4}
$T'_{i,t}$	a_1	2.126	0.57	3.713	2.3×10^{-4}
$P'_{i,t}$	a_2	1.189×10^{-2}	4.186×10^{-3}	2.841	4.69×10^{-3}
$T'_{i,t}^2$	a_3	-4.246×10^{-2}	1.196×10^{-2}	-3.549	4.25×10^{-4}
$P'_{i,t}^2$	a_4	-2.878×10^{-5}	1.115×10^{-5}	-2.581	1.01×10^{-2}
$\ln(I'_{i,t})$	α	0.741	3.281×10^{-2}	22.58	$< 2 \times 10^{-16}$

Table 1: Significance tests of terms in the regression (eqns. (5)-(7)) of log incidence ($\ln(I_{i,t})$) on temperature ($T'_{i,t}$), precipitation ($P'_{i,t}$), and a weighted average of log incidence in the previous five weeks ($\ln(I'_{i,t})$).

374 **Figures**

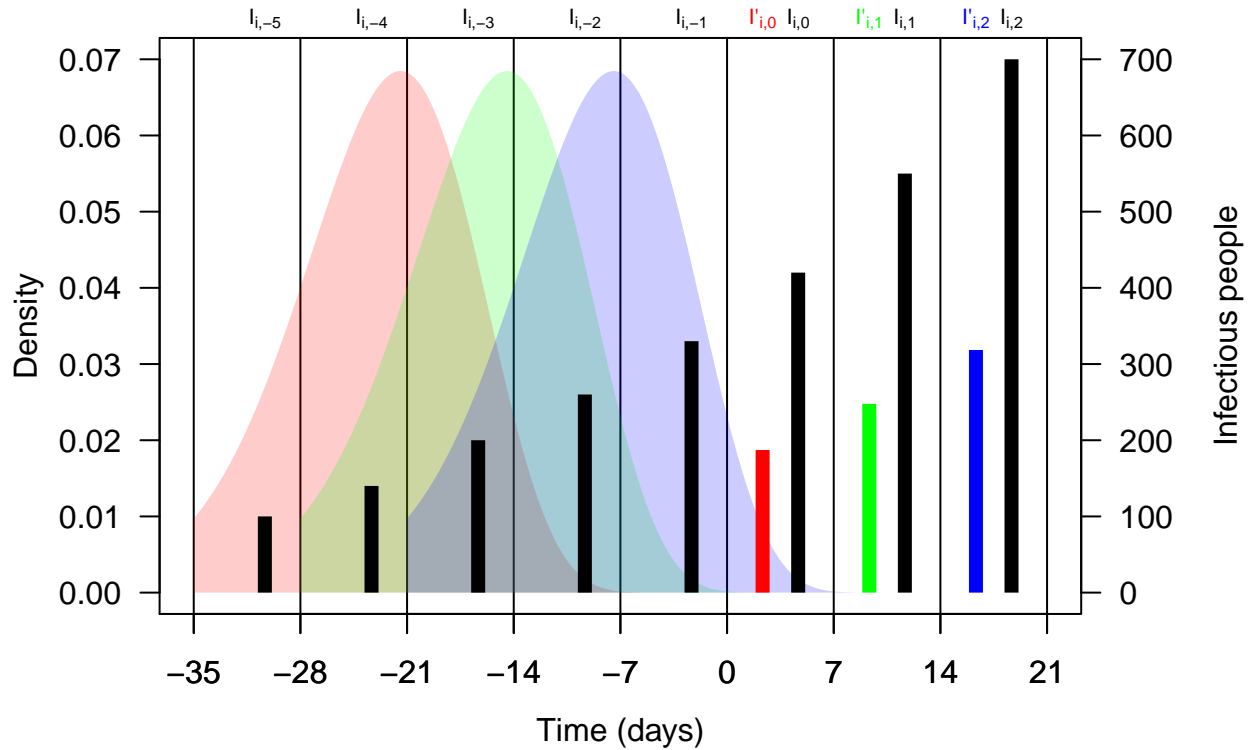


Figure 1: Schematic representation of the calculation of effective numbers of infectious people, $I'_{i,t}$. Black bars represent observed weekly case numbers, and red, green, and blue bars in weeks 0-2 represent effective numbers of infectious people in three consecutive weeks. Colored shapes show the serial interval distributions used in the calculation of ω_n and then in the calculation of $I'_{i,t}$ in each of weeks 0-2. Weekly case numbers were chosen for pedagogical purposes and do not reflect empirical data.

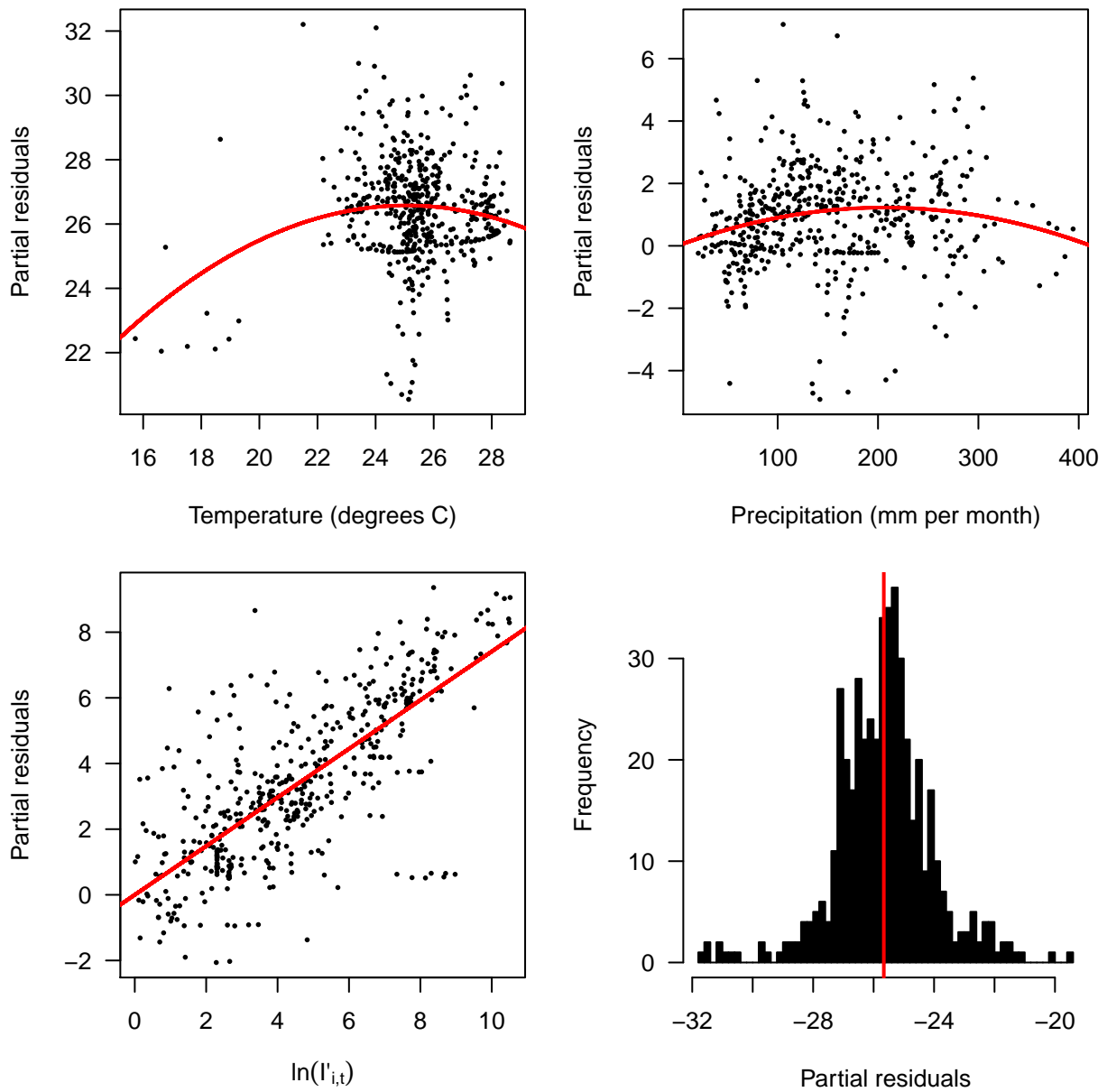


Figure 2: Partial residual plots of the fitted regression for temperature (top left), precipitation (top right), $\ln(I'_{i,t})$ (bottom left), and the intercept (bottom right).

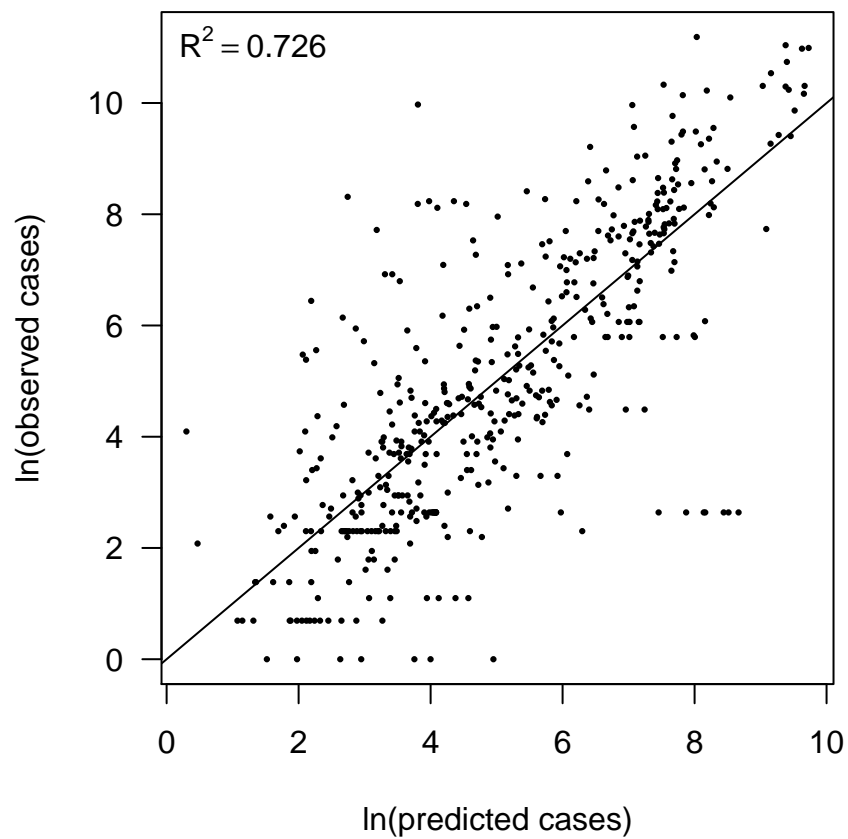


Figure 3: Relationship between predicted and observed cases in 484 country-weeks on a log-log scale. The line shows a one-to-one relationship for context.

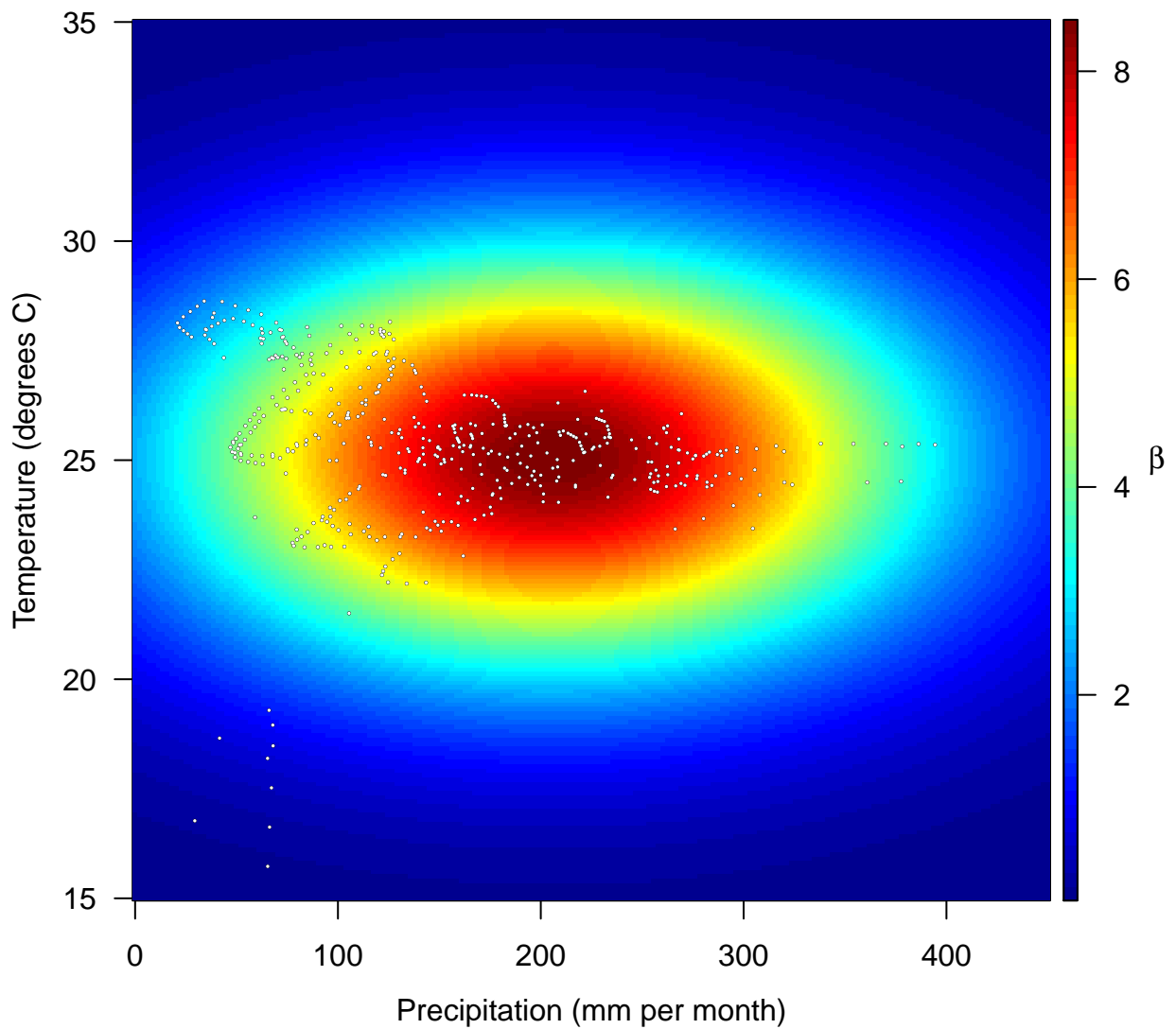


Figure 4: Fitted relationship for $f(T_{i,t}, P_{i,t})$, which models the influence of weekly mean temperature and precipitation on the transmission coefficient $\beta_{i,t}$. Points show temperature and precipitation values associated with country-weeks with positive incidence that were used in the regression.

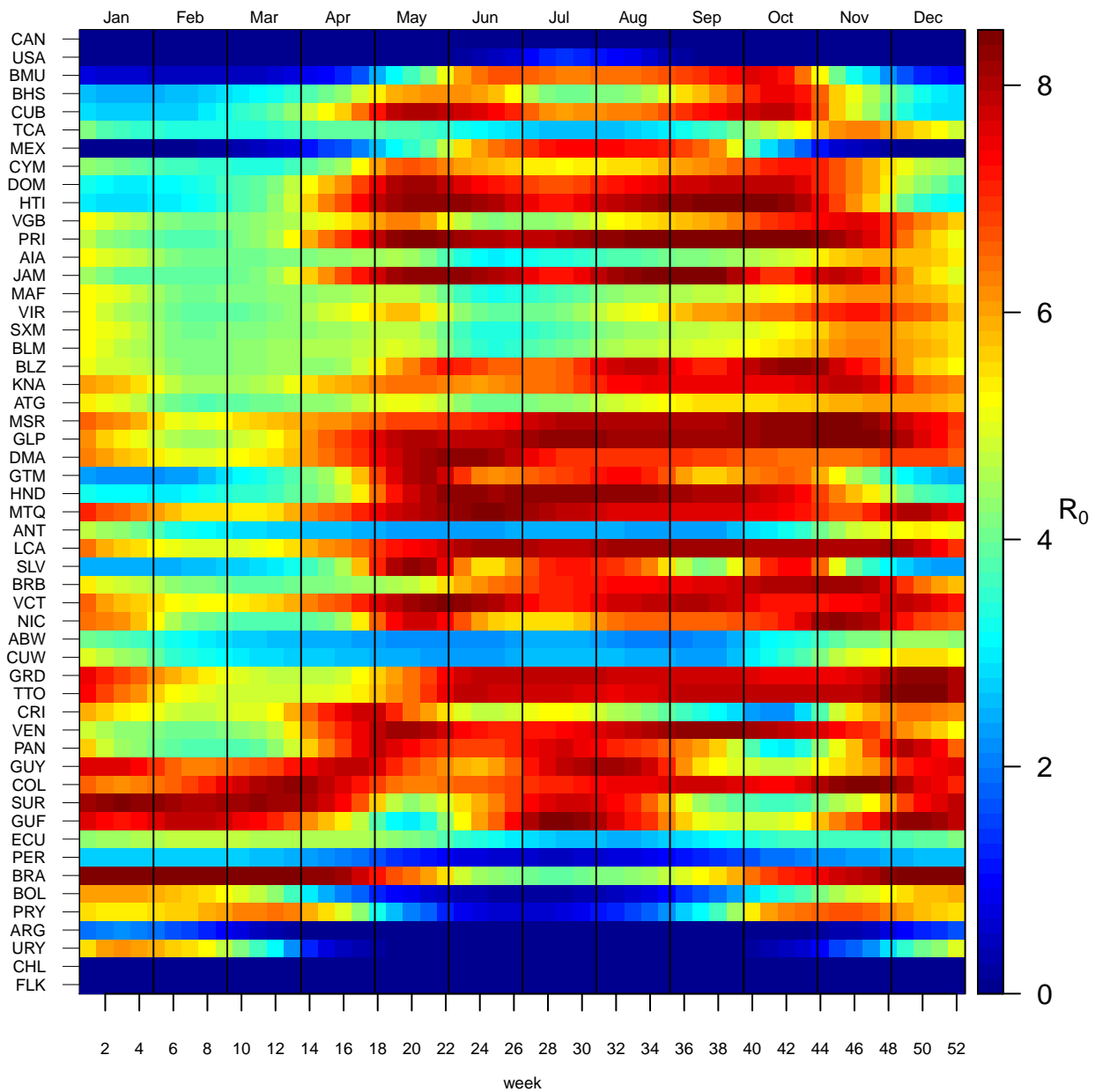


Figure 5: Seasonal patterns of predicted weekly R_0 by country. Countries are sorted by the latitudes of their capital cities.

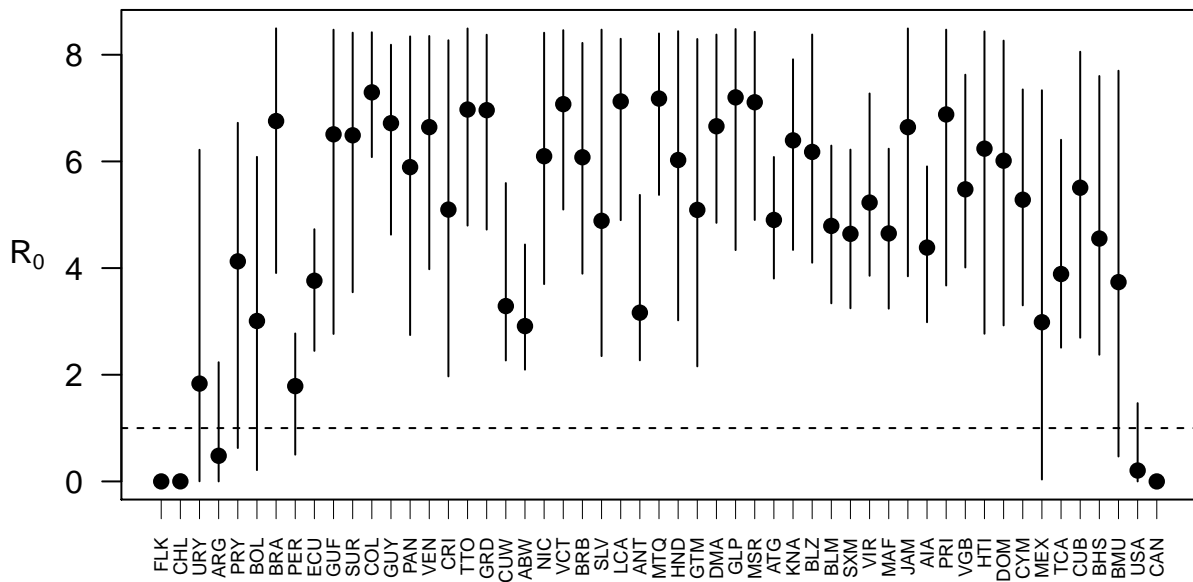


Figure 6: Variation in the range of weekly values of R_0 by country. Points show mean values across the year and line segments span the ranges of weekly values. Countries are sorted by the latitudes of their capital cities.

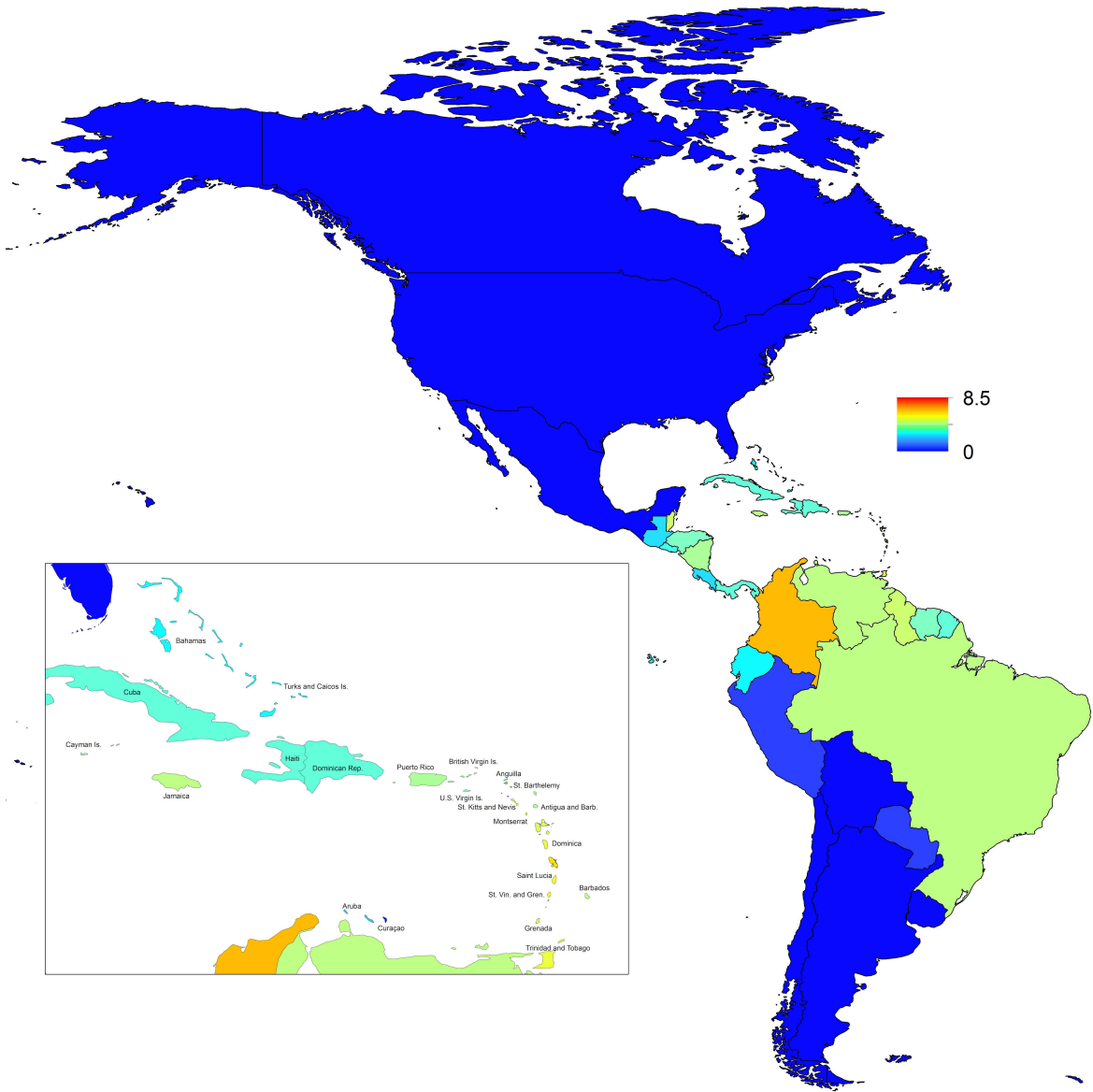


Figure 7: Map indicating the minimum weekly value of R_0 over a typical year for each of 53 countries.

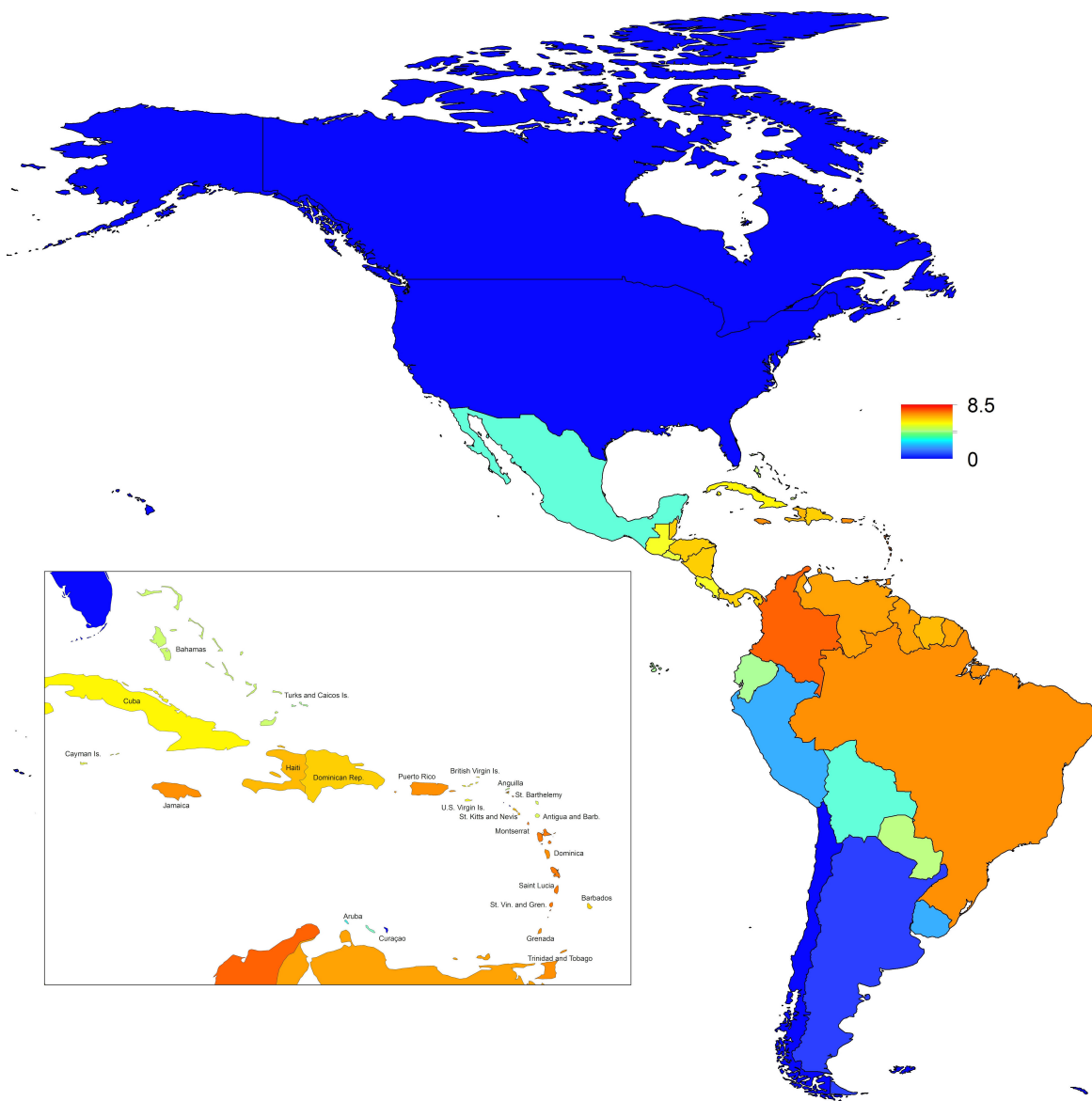


Figure 8: Map indicating the mean weekly value of R_0 over a typical year for each of 53 countries.

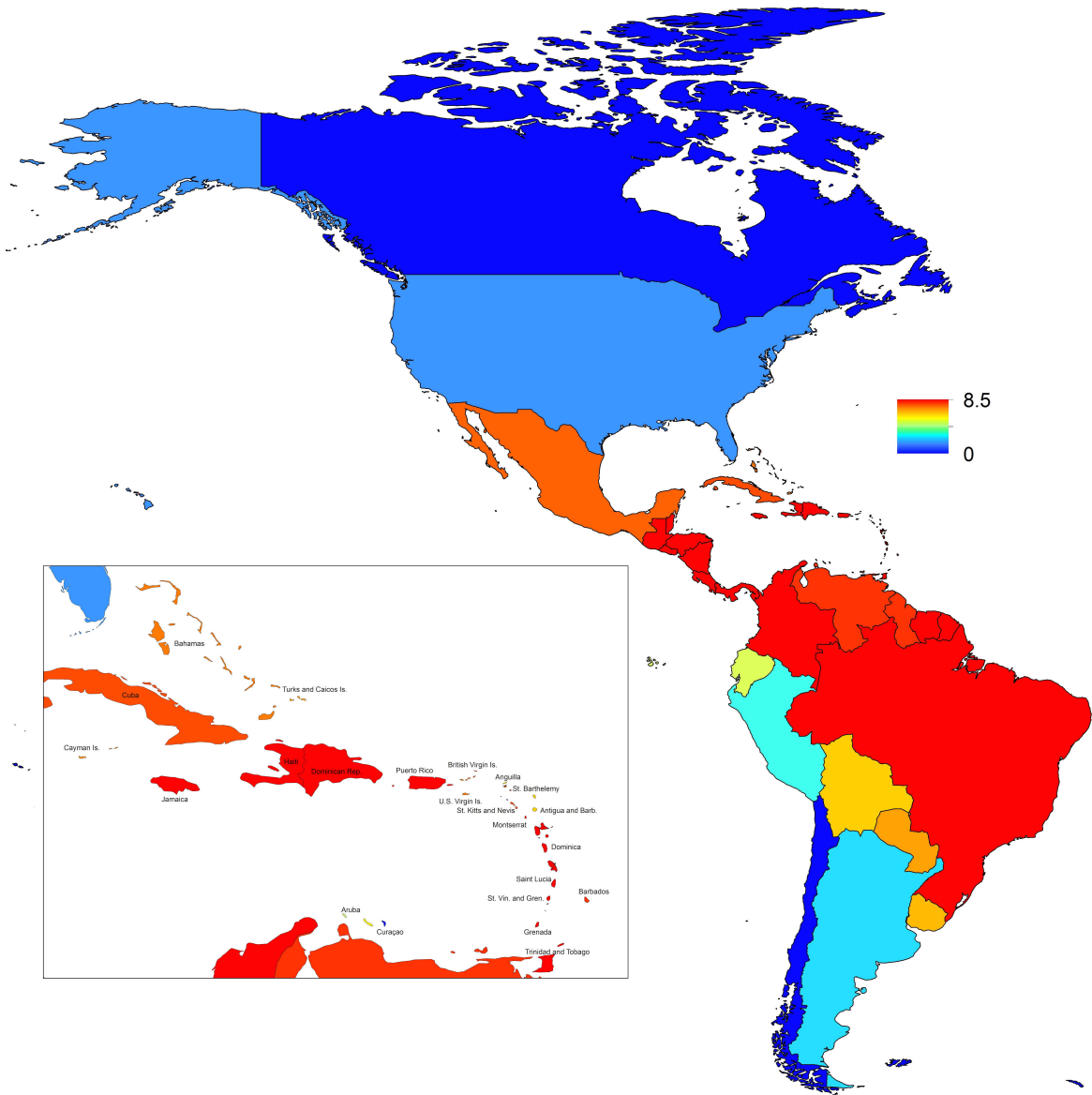


Figure 9: Map indicating the maximum weekly value of R_0 over a typical year for each of 53 countries.